iScience

CellPress
OPEN ACCESS

Article

# Dopamine neuron stimulation induces context-dependent abnormal involuntary movements in healthy rats

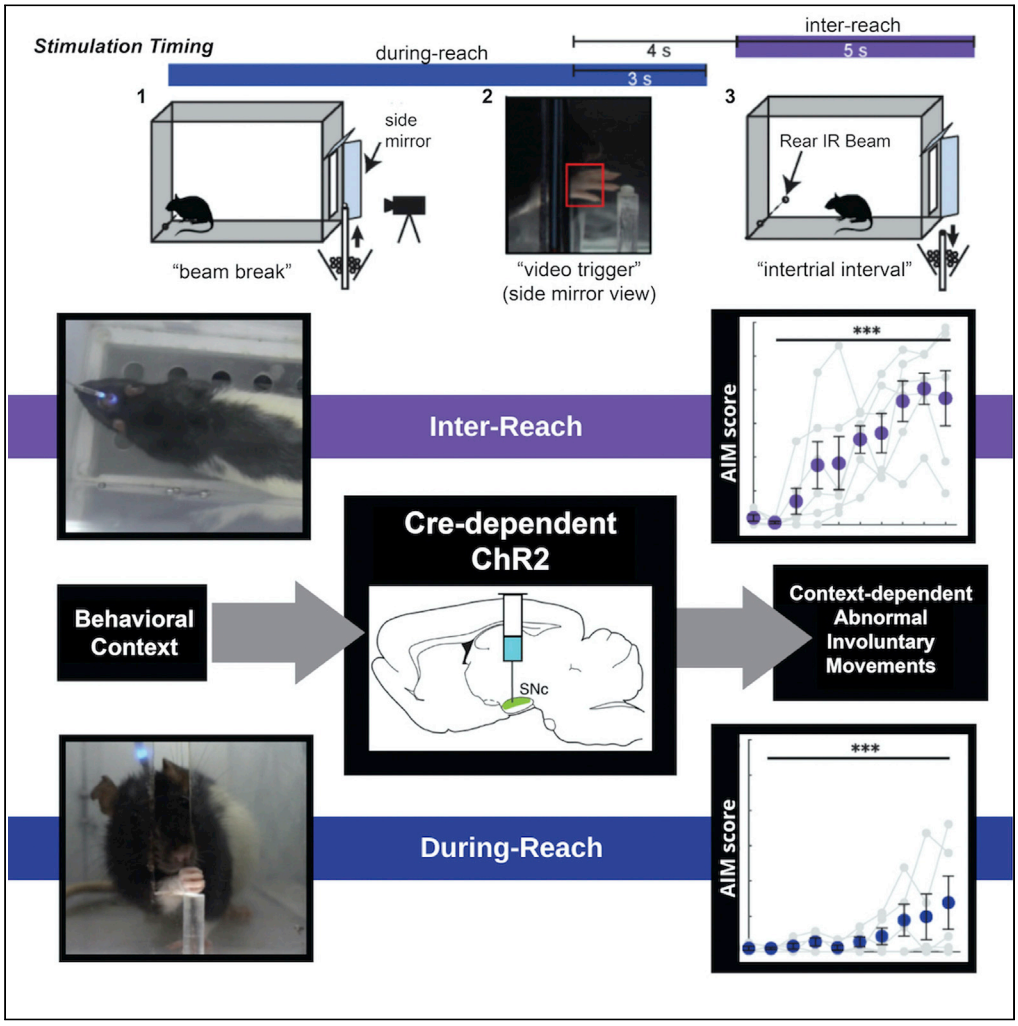


Julia Hunter, Alexandra Bova, Andrew Stevens, Daniel K. Leventhal

dleventh@med.umich.edu

## Highlights

Repeated dopamine neuron activation causes involuntary movements in healthy rats

These movements resemble levodopa-induced dyskinesias in parkinsonian rats

Movement severity depends on the history of prior stimulation

Movement severity is diminished in rats actively engaged in goal-directed behavior

Hunter et al., iScience 25, 103974
March 18, 2022 © 2022 The Authors.
https://doi.org/10.1016/j.isci.2022.103974

iScience

CellPress
OPEN ACCESS

Article

# Dopamine neuron stimulation induces context-dependent abnormal involuntary movements in healthy rats

Julia Hunter,[1] Alexandra Bova,[2] Andrew Stevens,[1] and Daniel K. Leventhal[1,3,4,5,6,*]

## SUMMARY

**With continued levodopa treatment, most patients with Parkinson disease (PD) develop levodopa-induced dyskinesias (LIDs)—abnormal involuntary movements (AIMs) characterized primarily by chorea. Clinically, LIDs depend on nigrostriatal degeneration and sensitization to repeated levodopa doses. However, the degree of dopamine denervation is correlated with levodopa-induced changes in striatal dopamine. Therefore, pulsatile dopamine release may induce AIMs independently of nigrostriatal degeneration. We optogenetically stimulated dopamine neurons in healthy rats as they engaged in skilled reaching. Repeated stimulation induced progressive AIMs whose severity was modified by behavioral context. AIMs were milder with stimulation during reaches, and more severe if stimulation occurred between reaches. Despite gradual induction, AIMs recurred immediately with subsequent dopamine neuron stimulation. Thus, nigrostriatal denervation is not necessary for fluctuating striatal dopamine to induce AIMs, and behavioral context modulates AIM expression. Furthermore, pulsatile dopamine release induces persistent changes in motor circuits that are revealed by subsequent dopamine neuron activation in appropriate contexts.**

## INTRODUCTION

Parkinson disease (PD) is characterized by slowness of movement (bradykinesia), rigidity, postural instability, and tremor. The primary treatment for PD is replacement of the dopamine depleted by substantia nigra pars compacta (SNc) degeneration. Levodopa is extremely effective in early PD, particularly at improving bradykinesia and rigidity. However, with extended treatment and PD progression, levodopa induces abnormal involuntary movements (AIMs) known as levodopa-induced dyskinesias (LIDs). These include "peak-dose" and "diphasic" dyskinesias. Peak-dose dyskinesias occur as serum levodopa concentrations peak and are characterized primarily by chorea. Diphasic dyskinesias tend to have a more dystonic quality, occur as serum levodopa levels rise or fall, and are more difficult to manage (Espay et al., 2018).

LID development depends on the degree of nigrostriatal degeneration and chronic levodopa treatment. LIDs appear earlier and more prominently in patients with more severe PD (Di Monte et al., 2000), the rate of dyskinesia onset in MPTP-lesioned monkeys is impacted by the extent of SNc lesions (Jenner, 2008), and greater nigrostriatal degeneration makes 6-OHDA-treated rodents more prone to LIDs (Cenci and Crossman, 2018; Winkler et al., 2002). Additionally, humans with MPTP intoxication developed dyskinesias shortly after levodopa initiation, some within six weeks (Langston, 2017). However, other studies suggest that nigrostriatal degeneration is not necessary for LID development. Healthy squirrel monkeys or macaques treated with repeated high-dose levodopa developed progressive dyskinesias (Pearce et al., 2001; Togasaki et al., 2001), though higher doses were necessary than in dopamine-depleted nonhuman primates.

Chronic levodopa treatment is also critical for LID induction and expression. The first dose of levodopa typically does not produce dyskinesias. In a majority of patients with PD, LIDs develop gradually, becoming more prominent with continuing treatment (Fahn, 2006). The same is true in the MPTP nonhuman primate and rodent 6-OHDA models. LIDs occur earlier and more intensely with higher levodopa doses, but almost never with the first dose (Cenci and Crossman, 2018; Lane et al., 2011; Lindgren et al., 2007; Pearce et al., 1995; Winkler et al., 2002).

[1]Department of Neurology, University of Michigan, Ann Arbor, MI 48109, USA

[2]Neuroscience Graduate Program, University of Michigan, Ann Arbor, MI 48109, USA

[3]Department of Biomedical Engineering, University of Michigan, Ann Arbor, MI 48109, USA

[4]Parkinson Disease Foundation Research Center of Excellence, University of Michigan, Ann Arbor, MI 48109, USA

[5]Department of Neurology, VA Ann Arbor Health System, Ann Arbor, MI 48105, USA

[6]Lead contact

*Correspondence: dleventh@med.umich.edu

https://doi.org/10.1016/j.isci.2022.103974


This is an open access article under the CC BY-NC-ND license (http://creativecommons.org/licenses/by-nc-nd/4.0/).

LID induction and expression are impacted not only by pharmacological priming but also by the behavioral context in which priming occurs (Lane et al., 2011). Similar to psychostimulant sensitization, placing an animal in a context in which LIDs were previously induced is sufficient to evoke dyskinesias (context-dependent conditioning) (Fornai et al., 2009). Furthermore, once AIMs have been induced in one context, they are reduced when levodopa is administered in a novel environment (context-dependent sensitization) (Lane et al., 2011). Finally, persons with PD often can perform activities of daily living despite moderate LIDs, suggesting that goal-directed movement at least partially overrides LID expression.

To determine the effects of context-specific striatal dopamine fluctuations independently of nigrostriatal degeneration, we repeatedly stimulated dopamine neurons in healthy rats as they performed single pellet skilled reaching. While not specifically modeling clinical LIDs, this approach allowed us to test three hypotheses relevant to LID pathogenesis. The first is that artificial dopamine neuron stimulation is sufficient to induce AIMs, even in dopamine-intact animals. The second is that AIMs expression depends on the physical context in which they were induced and tested. The third is that AIMs expression depends on behavioral context—the specific task in which the rat is engaged during dopamine neuron stimulation. AIMs strongly resembling levodopa-induced AIMs in dopamine-depleted rodents, developed with repeated dopamine neuron stimulation. Furthermore, AIM intensity depended on whether rats were engaged in skilled reaching during stimulation, with reaching mitigating AIM intensity.

## RESULTS

We optogenetically stimulated SNc dopamine neurons during and after rat skilled reaching. TH-Cre + rats were injected bilaterally with channelrhodopsin-EYFP fusion (ChR2) or control EYFP constructs (Figure 1). EYFP and TH expression overlapped strongly in the nigrostriatal pathway (Figure S1). Rats were then trained in an automated skilled reaching chamber (Bova et al., 2019; Ellens et al., 2016). In an individual trial, a rat breaks a photobeam at the back of the chamber, causing a pellet to lift in front of the reaching slot ("beam break", Figure 1D). The pellet remains lifted until 2 s after the rat breaches the reaching slot ("video trigger," Figure 1D). After rats completed training, we implanted an optical fiber over SNc contralateral to the rat's preferred reaching paw. Opsin expression was restricted to TH-expressing neurons in SNc projecting to striatum, and nigrostriatal TH expression was preserved (Figure S1, Bova et al., 2020).

### AIMs increase with repeated dopamine neuron stimulation

Rats received about 5 s of dopamine neuron stimulation per reach during ten 30-min sessions (Figure 1D). One group received stimulation from just before to just after reaches ("during-reach"), and a second group received stimulation only when the rat was not reaching ("inter-reach"). Control rats received the "during-reach" pattern of light administration, but had been injected with the EYFP-only construct. For this analysis, AIMs were evaluated only when the rat was not reaching ("non-reaching" Assessment Timing in Figure 1D). Baseline global AIMs scores in the reaching chamber did not differ significantly between groups (Kruskal-Wallis, matlab *kruskalwallis*: $X^2(1) = 0.51$, $p = 0.7752$). Both inter-reach and during-reach stimulation increased limb and axial AIM scores across sessions (Figure 2, Video S1). In control rats, no AIMs developed. Therefore, AIM severity increases gradually in response to repeated dopamine neuron stimulation. This is distinct from locomotor sensitization seen with amphetamine administration, as we observed abnormal forelimb and neck torsion similar to rodent LIDs (Crombag et al., 2001).

### AIM intensity is influenced by behavioral context

Because we observed AIMs during "non-reaching" stimulation epochs, we asked if AIMs also developed during the reaches themselves ("reaching"). Randomly selected "reach" videos from testing day 10 were scored. The global AIMs score was lower in the context of a reach than at other times in the reaching chamber (Figures 3A–3C, Videos S2 and S3). Therefore, AIMs severity depended on behavioral context in addition to the history of prior dopamine neuron activation.

In addition to differences in AIMs between "reaching" and "non-reaching" epochs, "non-reaching" AIMs were more severe with inter-reach than during-reach stimulation (Figure 3D). This is despite the fact that the duration of stimulation was similar for both groups, with a median during-reach stimulation duration of 5.37 s and a median inter-reach stimulation duration of 5 s (Bova et al., 2020). This suggests two

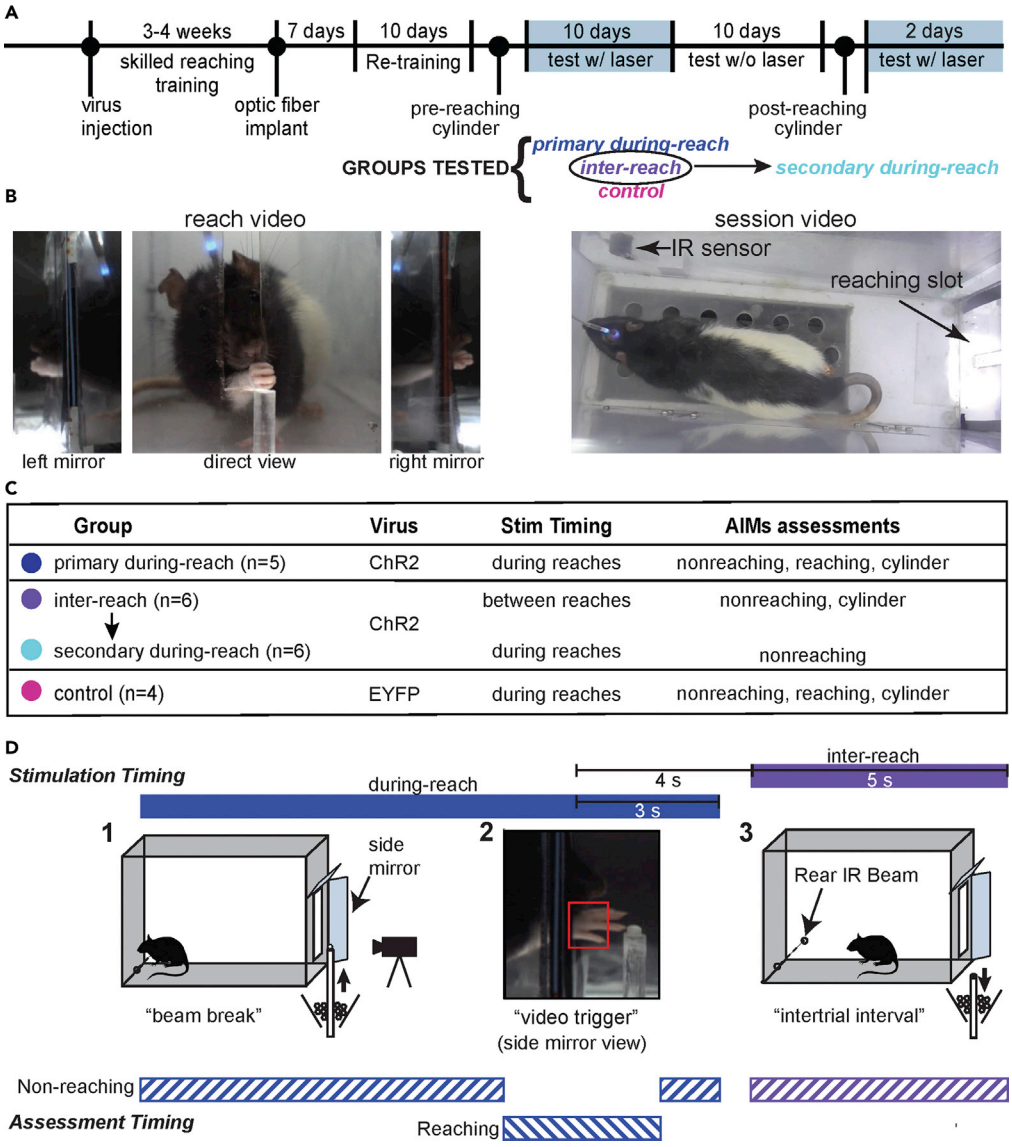


**Figure 1. Experimental design**

(A) Timeline for a single experiment. Only rats initially assigned to inter-reach stimulation received secondary during-reach stimulation.

(B) Video frames from "reach" and "session" videos. Individual reaches were recorded with a computer vision camera and angled mirrors. The entire session was recorded using a camcorder from the top of the chamber.

(C) Experimental groups. Rats were injected with either a ChR2-EYFP or EYFP-only viral construct, and assigned to one of two timings for optogenetic stimulation. n is the number of rats included in the analysis for each group (see STAR methods).

(D) A single skilled reaching trial. 1 – "beam break" – rat breaks IR beam at the back of the chamber to request a sugar pellet. 2 – "video trigger" – real-time analysis detects paw breaching the reaching slot to trigger 300 fps video from 1 s before to 3.33 s after the trigger event. 3 – "intertrial interval" – 2 s after the trigger event, the pellet delivery rod resets and the rat can initiate a new trial. Optogenetic manipulations occurred either "during-reach" (beam break to 3 s after video trigger) or "inter-reach" (beginning 4 s after video trigger and lasting 5 s). AIMs were assessed during laser-on periods either when the rat was actively reaching ("reaching", northwest-southeast stripes) or not ("non-reaching", southwest-northeast stripes).

See also Figure S1.

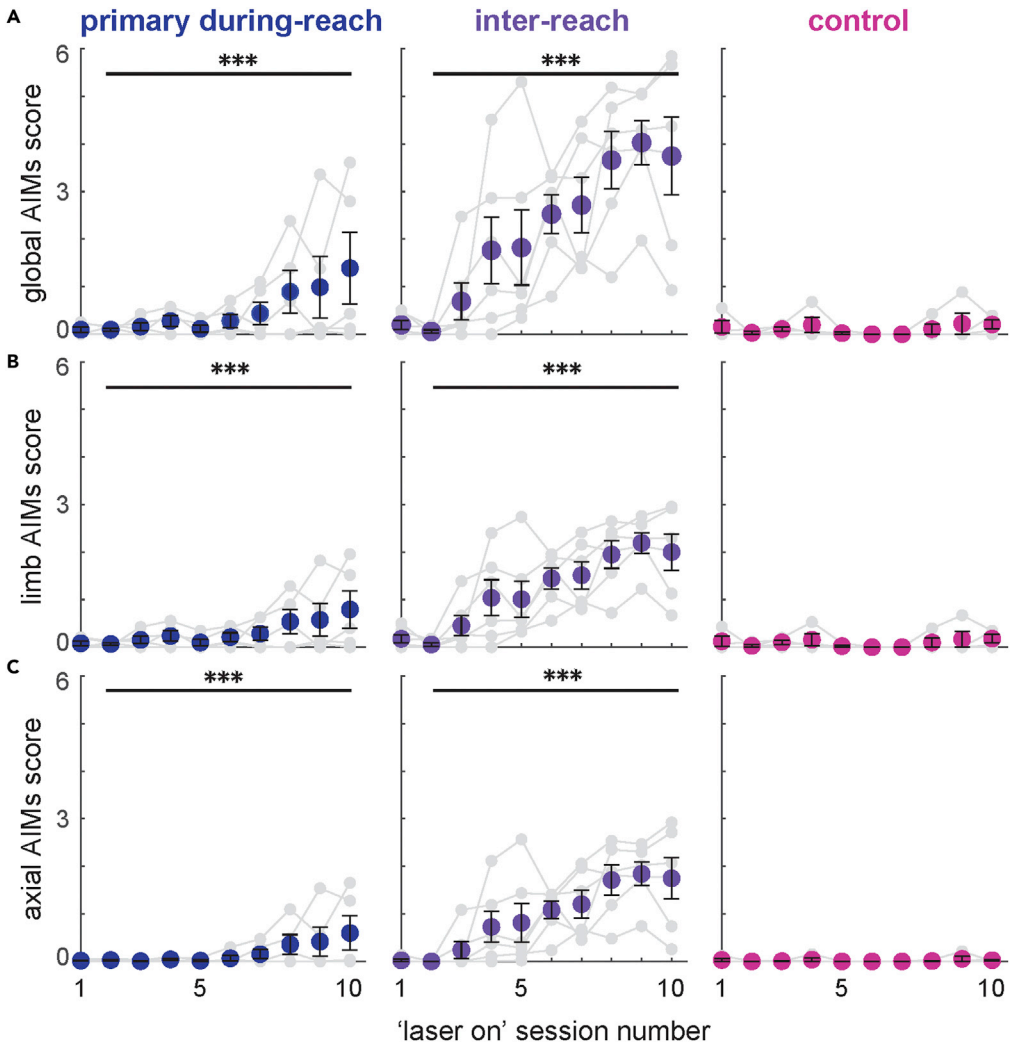


**Figure 2. AIMs scores progressively increased during non-reaching epochs during optogenetic stimulation of dopamine neurons**

Global (A), limb (B), and axial (C) AIMs scores for primary during-reach stimulation, inter-reach stimulation, and control rats during non-reaching epochs.

(A) Global AIMs score increased across sessions for during-reach and inter-reach stimulation. (During-reach: linear mixed model: interaction between session number and global AIMs score: $t(44) = 4.114$, $p = 0.000168$) (Inter-reach: linear mixed model: interaction between session number and global AIMs score: $t(53) = 10.961$, $p = 7.71e\text{-}15$) (Control: linear mixed model: interaction between session number and global AIMs score: $t(35) = 0.781$, $p = 0.440$).

(B) Limb AIMs score increased across sessions for during-reach and inter-reach stimulation. (During-reach: linear mixed model: interaction between session number and limb AIMs score: $t(44) = 4.087$, $p = 0.000183$) (Inter-reach: linear mixed model: interaction between session number and limb AIMs score: $t(53) = 10.858$, $p = 4.37e\text{-}15$) (Control: linear mixed model: interaction between session number and limb AIMs score: $t(35) = 0.803$, $p = 0.427$).

(C) Axial AIMs scores increased across sessions for during-reach and inter-reach stimulation. (During-reach: linear mixed model: interaction between session number and axial AIMs score: $t(44) = 4.030$, $p = 0.000218$) (Inter-reach: linear mixed model: interaction between session number and axial AIMs score: $t(53) = 10.237$, $p = 3.69e\text{-}14$) (Control: linear mixed model: interaction between session number and axial AIMs score: $t(35) = 0.613$, $p = 0.544$).

***$p < 0.001$. Data are represented as mean ± SEM.

See also Video S1.

non-exclusive possibilities: AIM induction is suppressed by reaching and/or AIM expression is suppressed by reaching. To test the possibility that behavioral context influences AIM expression, we compared AIM scores in rats that had received 10 days of inter-reach stimulation, and then switched to during-reach stimulation ('secondary during' stimulation). Non-reaching AIM scores decreased in the during-reach

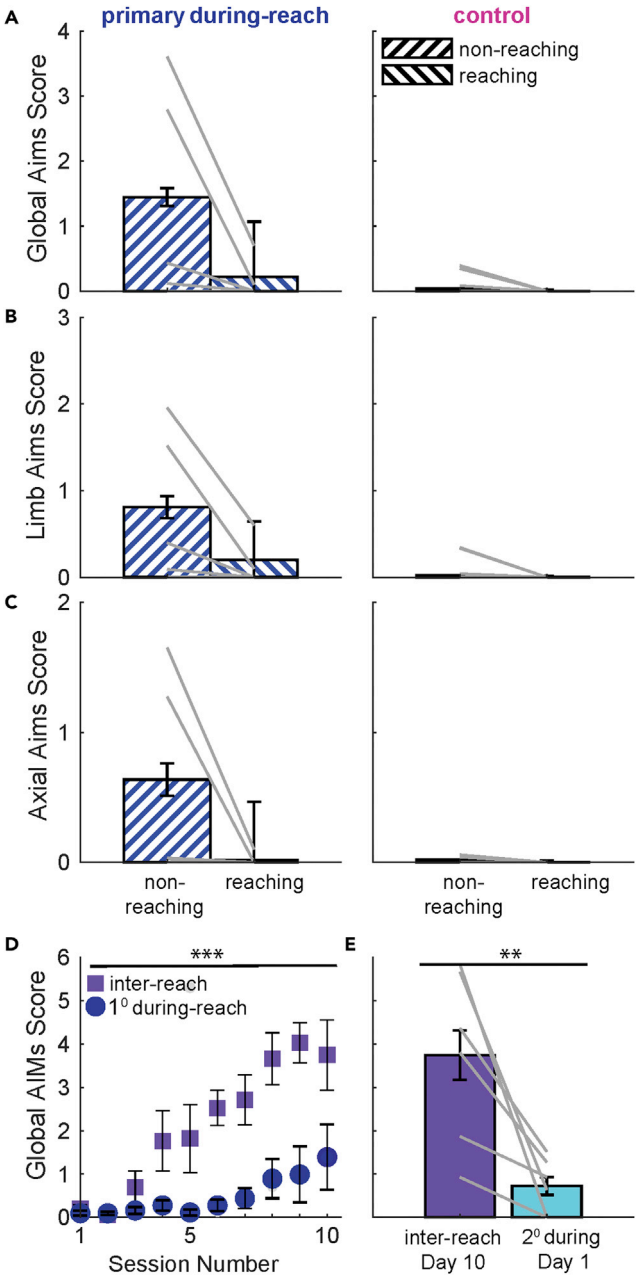


**Figure 3. AIMs are more severe when rats are not actively engaged in the skilled reaching task**

Comparison of global (A), limb (B), and axial (C) AIMs scores between non-reaching and reaching epochs for primary during-reach stimulation and control rats.

(A) (Primary During-reach: Wilcoxon Signed-Rank: W = 0, p = 0.25) (Control: Wilcoxon Signed-Rank: W = 0, p = 0.1250).

(B) (Primary During-reach: Wilcoxon Signed-Rank: W = 0, p = 0.1250) (Control: Wilcoxon Signed-Rank: W = 0, p = 0.2500).

(C) (Primary During-reach: Wilcoxon Signed-Rank: W = 0, p = 0.1250) (Control: Wilcoxon Signed-Rank: W = 0, p = 0.4286).

(D) Comparison of global AIMs scores during non-reaching epochs for during-reach and inter-reach stimulation (these are the same data as in Figure 2A repeated here on the same axes for clarity). There was a significant difference in the effect of group on AIMs development (linear mixed model: interaction effects of group and session number on global AIMs score: $t(97) = 5.945$, $p = 4.35 \times 10^{-8}$).

(E) Comparison of non-reaching global AIMs scores for inter-reach stimulation day 10 and secondary during-reach stimulation day 1 sessions (Wilcoxon Signed-Rank: W = 21, p = 0.0313). AIMs were more severe during non-reaching epochs when rats are not actively engaged in the reaching task or approaching the reaching slot.

**p <0.01; ***p <0.001. Data are represented as mean ± SEM.

See also Videos S2 and S3.

stimulation sessions (Figure 3E, Video S3). This suggests that goal-directed movement mitigates AIM expression because during-reach stimulation occurred mainly as the rat approached the reaching slot (Figure 3E).

### Changing physical context did not mitigate AIMs expression

We next asked if AIMs were influenced by the physical environment in which rats received dopamine neuron stimulation. After 10 days of skilled reaching, we placed rats in a clear cylinder and stimulated SNc (Figure 4 and Video S4). We compared day 10 "primary during-reach" and "inter-reach" AIMs scores to "cylinder" context AIM scores. We predicted that AIMs would decrease with stimulation outside of the reaching chamber. However, changes in AIMs scores were inconsistent at the level of individual rats, and only limb AIMs for rats that had received inter-reach stimulation decreased significantly.

## DISCUSSION

Our goal was to determine the ability of optogenetic SNc dopamine neuron stimulation in healthy rats to generate AIMs in different behavioral and physical contexts. Our results support four conclusions: first, AIMs can be produced by dopamine neuron stimulation in healthy rats, indicating that nigrostriatal degeneration is not necessary to induce dopamine-dependent AIMs. Second, AIMs are sensitized by repeated dopamine neuron stimulation. Third, behavioral context influences AIM expression. Finally, while behavioral context (i.e., what one is doing) clearly plays a role in AIM expression, the effects of physical context (where one is doing it) are less certain.

Nigrostriatal degeneration causes many anatomic and physiologic changes that likely contribute to LID pathogenesis (Simon et al., 2020). The appearance of AIMs in healthy rats, however, argues that nigrostriatal degeneration is not necessary for AIM induction. This is consistent with observations in dopamine-intact nonhuman primates, who develop dyskinesias if given sufficiently high levodopa doses (Pearce et al., 2001; Togasaki et al., 2001). There are several potential explanations for these findings. First, the AIMs we observed may be phenomenologically distinct from levodopa-induced AIMs in 6-OHDA-lesioned rats. However, AIMs in rat LID models and in our rats look very similar, at least to the extent that one can make phenomenological distinctions in rodents. Second, the magnitude of striatal dopamine fluctuations may be the major determinant of dyskinesias, rather than network changes caused by SNc degeneration. In support of this idea, changes in striatal dopamine in response to levodopa depend strongly on nigrostriatal degeneration. For example, high levodopa doses (100 mg/kg) modestly increase striatal dopamine in healthy rats, but the same dose in 6-OHDA-lesioned rats causes a much (~10x) larger increase (Abercrombie et al., 1990). In humans with PD, disease duration is correlated with changes in $^{11}$C-raclopride binding potential in PET images, a surrogate for dopamine receptor occupancy (de la Fuente-Fernández et al., 2004). This again suggests that the severity of nigrostriatal degeneration determines the magnitude of striatal dopamine changes in response to a fixed levodopa dose. Thus, dopamine denervation may accelerate LID induction by increasing the magnitude of striatal dopamine fluctuations, which acts in concert with synaptic/circuit-level changes due to chronic dopamine loss. The relative contributions of striatal dopamine fluctuations and network changes related to dopamine loss are therefore difficult to disentangle in a dopamine-depleted animal model.

Our comparative data between "reaching" and "non-reaching" epochs provide insight into the role of behavioral context in the development of dopamine-dependent AIMs. The effects of distinct settings (physical context) on psychomotor sensitization have been studied extensively (Lane et al., 2011). The difference in AIMs severity between "reaching" and "non-reaching" epochs indicates that behavioral context-specific sensitization also occurs. Rats exhibited few AIMs while reaching, even when AIMs scores were very high in "non-reaching" epochs or the "cylinder" context (Figure 3) (Bova et al., 2020). Optogenetically induced AIMs are sensitive to behavioral context: involvement in a goal-directed task decreases the severity of dyskinesia. This is consistent with the observation that human patients with PD often perform goal-directed movements despite moderate or even severe LIDs. Nonetheless, when AIMs were present during reaching (e.g., Video S2), they can interfere with goal-directed movements.

The fact that AIMs severity was higher for inter-reach than during-reach stimulation further argues that behavioral context is critical to the expression, and possibly induction, of dopamine-induced AIMs. When we later exposed the inter-reach stimulation group to "secondary during-reach" stimulation,

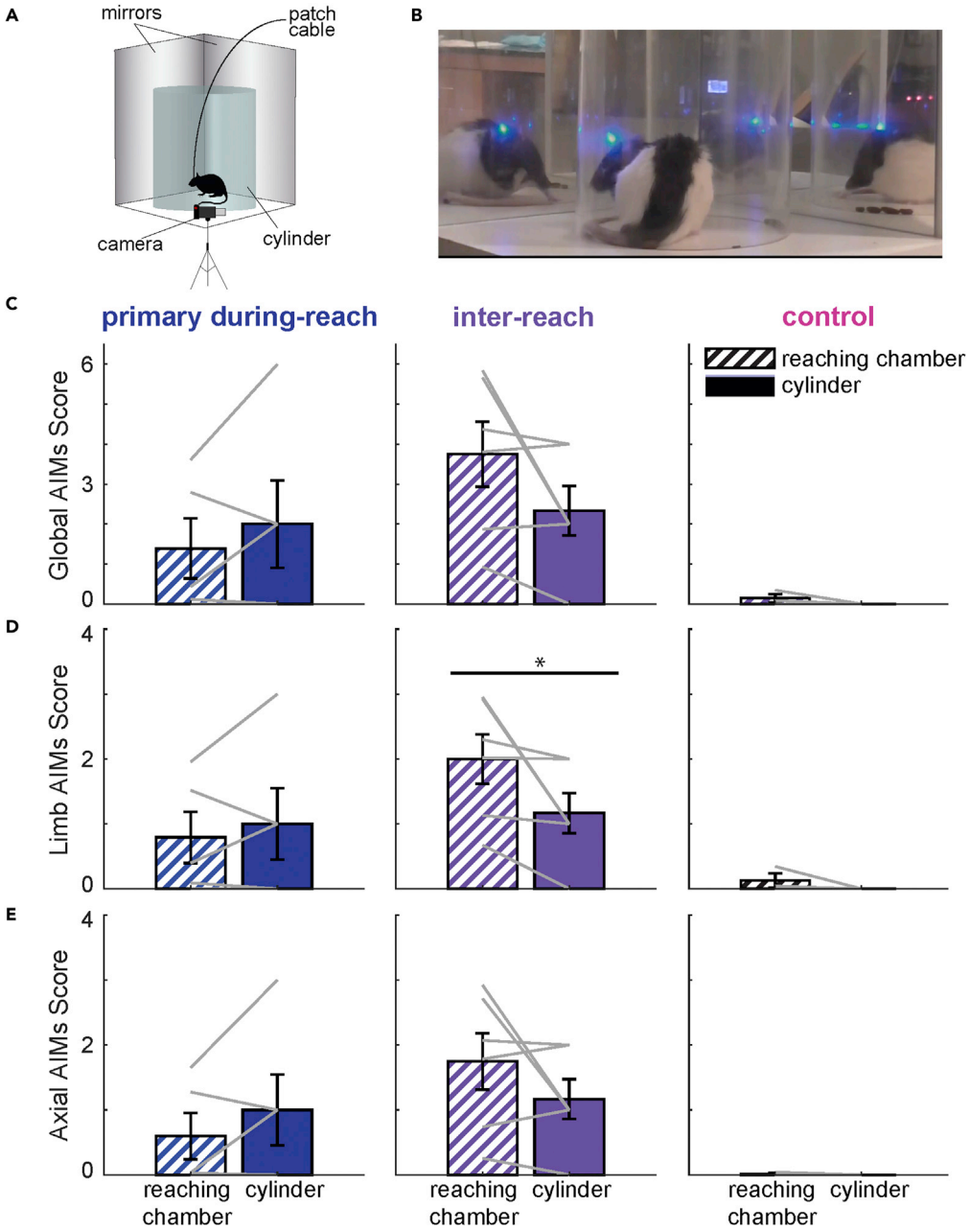


**Figure 4. AIMs scores are similar in the reaching chamber and cylinder contexts**

(A) Schematic of the apparatus for AIM measurement in the cylinder context.

(B) Still frame of a rat during optogenetic stimulation (Primary During-reach stimulation, ChR2).

(C–E) Comparison of global (C), limb (D), and axial (E) AIMs scores for non-reaching epochs during day 10 of stimulation in the skilled reaching chamber and in the "post-reaching" cylinder context (stimulation at estimated 20 mW at the fiber tip in both conditions). (C) Global AIMs score comparison between contexts: Primary During-reach: Wilcoxon Signed-Rank: $W = 3$, $p = 0.6250$. Inter-reach: Wilcoxon Signed-Rank: $W = 21$, $p = 0.0313$. Control: Wilcoxon Signed-Rank: $W = 3$, $p = 0.5$. (D) Limb AIMs score comparison between contexts: Primary During-reach: Wilcoxon Signed-Rank: $W = 3$, $p = 0.6250$. Inter-reach: Wilcoxon Signed-Rank: $W = 21$, $p = 0.0313$. Control: Wilcoxon Signed-Rank: $W = 3.5$, $p = 0.5$. (E) Axial AIMs score comparison between contexts: Primary During-reach: Wilcoxon Signed-Rank: $W = 3$, $p = 0.6250$. Inter-reach: Wilcoxon Signed-Rank: $W = 15$, $p = 0.4375$. Control: Wilcoxon Signed-Rank: $W = 1$, $p = 1.00$.

*$p < 0.1$. Data are represented as mean ± SEM.

See also Video S4.

AIMs severity significantly decreased (Figure 3E). This suggests that execution of goal-directed movements during periods of elevated striatal dopamine is sufficient to mitigate AIMs expression, though it is also possible that goal-directed behavior decreases stimulation-evoked dopamine release. This hypothesis would be difficult to test in 6-OHDA- or MPTP-lesioned animals. They would have to perform a single action for several hours after a levodopa dose while striatal dopamine remained elevated. Optogenetics in healthy animals allowed us to manipulate dopamine levels only while rats perform a specific action.

The minimal impact of physical context (reaching chamber vs. cylinder) suggests that it is less important than behavioral context in sensitization to dopamine neuron stimulation, with several caveats. First, if dopamine levels are high enough, severe AIMs might occur regardless of environment once induced (i.e., a ceiling effect). This is unlikely because AIMs were of mild to moderate severity in most rats. The opposite is also possible—that AIMs were so mild in the reaching chamber, that they could not decrease further (i.e., a floor effect). This also seems unlikely, because control rats had essentially zero AIMs. One potential confound is that these rats had already received stimulation once in the cylinder context. This one exposure could have stripped the cylinder of its novelty, or been sufficient to sensitize AIMs in this context (Crombag et al., 2001). Finally, the rats were actively engaged in a rewarding task in the reaching chamber, but not the cylinder. Task engagement by itself likely alters striatal dopamine levels, and therefore AIMs expression. Experiments dedicated to examining the influence of physical context on AIMs using truly novel environments with rats engaged in the same behavior while monitoring striatal dopamine levels would address these possibilities.

Because we directly stimulated SNc neurons, our results are almost certainly caused by transient, task-specific elevation of striatal dopamine. They therefore are likely relevant to the pathophysiology of peak-dose dyskinesias. This is further supported by the observation that AIMs in rodents treated with 6-OHDA and levodopa peak and ebb over a time course roughly matching brain dopamine concentrations (Carta et al., 2006; Lindgren et al., 2010), and are phenotypically similar to the AIMs we observed.

In summary, AIMs can be induced by nigrostriatal dopamine pathway activation in the absence of dopamine denervation. Context-specific AIMs sensitization may be more dependent on behavioral than physical context. Lastly, the ability of dopamine stimulation to express (and possibly induce) AIMs is decreased during goal-directed actions. These phenomena have clinical relevance in determining how best to utilize levodopa in ways that avoids disruptive motor complications.

### Limitations of the study

There are several limitations to this study. First, we did not completely isolate physical from behavioral context-specific sensitization, because reaching never occurred in the cylinder. Additionally, because we did not record dopamine levels, it is unclear how the magnitude of dopamine release influences AIM sensitization or compares to dopamine levels achieved during LIDs.

## STAR★METHODS

Detailed methods are provided in the online version of this paper and include the following:

- KEY RESOURCES TABLE
- RESOURCE AVAILABILITY
  - Lead contact
  - Materials availability
  - Data and code availability
- EXPERIMENTAL MODEL AND SUBJECT DETAILS
- METHOD DETAILS
  - Virus injections and surgeries
  - Skilled reaching
  - Optogenetics
  - Dopamine neuron stimulation in the cylinder context
  - AIMs scoring
  - Behavioral conditions

- Immunohistochemistry
- QUANTIFICATION AND STATISTICAL ANALYSIS

## SUPPLEMENTAL INFORMATION

Supplemental information can be found online at https://doi.org/10.1016/j.isci.2022.103974.

## ACKNOWLEDGMENTS

The authors would like to thank Dr. Roger Albin for reading earlier versions of the manuscript and his constructive advice. This work was funded by NIH K08-NS072183, NIH P50-NS091856, NIH R56-NS109227, NIH R01-NS109227, a Brain Research Foundation Seed Grant, and the University of Michigan Parkinson Foundation Research Center of Excellence grant.

## AUTHOR CONTRIBUTIONS

JH performed the experiments, analyzed the data, and drafted the manuscript. AB designed and performed the experiments, and analyzed the data. AS assisted with data analysis. DKL designed the experiments, interpreted the data, and drafted the manuscript with JH.

## DECLARATION OF INTERESTS

The authors declare no competing interests.

Received: October 14, 2021
Revised: January 5, 2022
Accepted: February 18, 2022
Published: March 18, 2022

## REFERENCES

Abercrombie, E.D., Bonatz, A.E., and Zigmond, M.J. (1990). Effects of L-dopa on extracellular dopamine in striatum of normal and 6-hydroxydopamine-treated rats. Brain Res. *525*, 36–44. https://doi.org/10.1016/0006-8993(90)91318-b.

Bova, A., Gaidica, M., Hurst, A., Iwai, Y., Hunter, J., and Leventhal, D.K. (2020). Precisely timed dopamine signals establish distinct kinematic representations of skilled movements. Elife *9*. https://doi.org/10.7554/eLife.61591.

Bova, A., Kernodle, K., Mulligan, K., and Leventhal, D. (2019). Automated rat single-pellet reaching with 3-dimensional reconstruction of paw and digit trajectories. J. Vis. Exp. e59979. https://doi.org/10.3791/59979.

Carta, M., Lindgren, H.S., Lundblad, M., Stancampiano, R., Fadda, F., and Cenci, M.A. (2006). Role of striatal L-DOPA in the production of dyskinesia in 6-hydroxydopamine lesioned rats. J. Neurochem. *96*, 1718–1727. https://doi.org/10.1111/j.1471-4159.2006.03696.x.

Cenci, M.A., and Crossman, A.R. (2018). Animal models of l-dopa-induced dyskinesia in Parkinson's disease. Mov. Disord. *33*, 889–899. https://doi.org/10.1002/mds.27337.

Crombag, H.S., Badiani, A., Chan, J., Dell'Orco, J., Dineen, S.P., and Robinson, T.E. (2001). The ability of environmental context to facilitate psychomotor sensitization to amphetamine can be dissociated from its effect on acute drug responsiveness and on conditioned responding. Neuropsychopharmacology *24*, 680–690. https://doi.org/10.1016/s0893-133x(00)00238-4.

de la Fuente-Fernández, R., Sossi, V., Huang, Z., Furtado, S., Lu, J.-Q., Calne, D.B., Ruth, T.J., and Stoessl, A.J. (2004). Levodopa-induced changes in synaptic dopamine levels increase with progression of Parkinson's disease: implications for dyskinesias. Brain *127*, 2747–2754. https://doi.org/10.1093/brain/awh290.

Di Monte, D.A., McCormack, A., Petzinger, G., Janson, A.M., Quik, M., and Langston, W.J. (2000). Relationship among nigrostriatal denervation, parkinsonism, and dyskinesias in the MPTP primate model. Mov Disord. *15*, 459–466. https://doi.org/10.1002/1531-8257(200005)15:3<459::Aid-mds1006>3.0.Co;2-3.

Ellens, D.J., Gaidica, M., Toader, A., Peng, S., Shue, S., John, T., Bova, A., and Leventhal, D.K. (2016). An automated rat single pellet reaching system with high-speed video capture. J. Neurosci. Methods *271*, 119–127. https://doi.org/10.1016/j.jneumeth.2016.07.009.

Espay, A.J., Morgante, F., Merola, A., Fasano, A., Marsili, L., Fox, S.H., Bezard, E., Picconi, B., Calabresi, P., and Lang, A.E. (2018). Levodopa-induced dyskinesia in Parkinson disease: current and evolving concepts. Ann. Neurol. *84*, 797–811. https://doi.org/10.1002/ana.25364.

Fahn, S. (2006). Levodopa in the treatment of Parkinson's disease. J. Neural Transm. Suppl. In (Springer Vienna), pp. 1–15. https://doi.org/10.1007/978-3-211-33328-0_1.

Fornai, F., Biagioni, F., Fulceri, F., Murri, L., Ruggieri, S., and Paparelli, A. (2009). Intermittent Dopaminergic stimulation causes behavioral sensitization in the addicted brain and parkinsonism. Int. Rev. Neurobiol. *88*, 371–398. https://doi.org/10.1016/s0074-7742(09)88013-6.

Jenner, P. (2008). Molecular mechanisms of L-DOPA-induced dyskinesia. Nat. Rev. Neurosci. *9*, 665–677. https://doi.org/10.1038/nrn2471.

Lane, E.L., Daly, C.S., Smith, G.A., and Dunnett, S.B. (2011). Context-driven changes in L-DOPA-induced behaviours in the 6-OHDA lesioned rat. Neurobiol. Dis. *42*, 99–107. https://doi.org/10.1016/j.nbd.2011.01.010.

Langston, J.W. (2017). The MPTP story. J. Parkinson's Dis. *7*, S11–S19. https://doi.org/10.3233/JPD-179006.

Lindgren, H.S., Andersson, D.R., Lagerkvist, S., Nissbrandt, H., and Cenci, M.A. (2010). L-DOPA-induced dopamine efflux in the striatum and the substantia nigra in a rat model of Parkinson's disease: temporal and quantitative relationship to the expression of dyskinesia. J. Neurochem. *112*, 1465–1476. https://doi.org/10.1111/j.1471-4159.2009.06556.x.

Lindgren, H.S., Rylander, D., Ohlin, K.E., Lundblad, M., and Cenci, M.A. (2007). The "motor complication syndrome" in rats with 6-OHDA lesions treated chronically with L-DOPA: relation to dose and route of administration. Behav. Brain Res. *177*, 150–159. https://doi.org/10.1016/j.bbr.2006.09.019.

Pearce, R.K., Heikkilä, M., Lindén, I.B., and Jenner, P. (2001). L-dopa induces dyskinesia in normal monkeys: behavioural and pharmacokinetic observations. Psychopharmacology (Berl) *156*, 402–409. https://doi.org/10.1007/s002130100733.

Pearce, R.K., Jackson, M., Smith, L., Jenner, P., and Marsden, C.D. (1995). Chronic L-DOPA administration induces dyskinesias in the 1-methyl-4- phenyl-1,2,3,6-tetrahydropyridine-treated common marmoset (Callithrix Jacchus). Mov. Disord. *10*, 731–740. https://doi.org/10.1002/mds.870100606.

Sebastianutto, I., Maslava, N., Hopkins, C.R., and Cenci, M.A. (2016). Validation of an improved scale for rating l-DOPA-induced dyskinesia in the mouse and effects of specific dopamine receptor antagonists. Neurobiol. Dis. *96*, 156–170. https://doi.org/10.1016/j.nbd.2016.09.001.

Simon, D.K., Tanner, C.M., and Brundin, P. (2020). Parkinson disease epidemiology, pathology, genetics, and pathophysiology. Clin. Geriatr. Med. *36*, 1–12. https://doi.org/10.1016/j.cger.2019.08.002.

Togasaki, D.M., Tan, L., Protell, P., Di Monte, D.A., Quik, M., and Langston, J.W. (2001). Levodopa induces dyskinesias in normal squirrel monkeys. Ann. Neurol. *50*, 254–257. https://doi.org/10.1002/ana.1099.

Winkler, C., Kirik, D., Björklund, A., and Cenci, M.A. (2002). L-DOPA-induced dyskinesia in the intrastriatal 6-hydroxydopamine model of Parkinson's disease: relation to motor and cellular parameters of nigrostriatal function. Neurobiol. Dis. *10*, 165–186. https://doi.org/10.1006/nbdi.2002.0499.

## STAR★METHODS

### KEY RESOURCES TABLE

| REAGENT or RESOURCE | SOURCE | IDENTIFIER |
|---|---|---|
| Antibodies | | |
| Anti-GFP (mouse monoclonal) | Millipore-Sigma | Cat. #: MAB3580; RRID: AB_94936 |
| Anti-TH (rabbit polyclonal) | Millipore-Sigma | Cat. #: AB152; RRID: AB_390204 |
| AF 488 donkey anti-mouse IgG | ThermoFisher | Cat. #:A-21202; RRID: AB_141607 |
| AF 555 donkey anti-rabbit IgG | ThermoFisher | Cat. #: A-31572; RRID: AB_162543 |
| Bacterial and virus strains | | |
| AAV5-EF1a-DIO-hChR2(H134R)-EYFP | UNC Vector Core | N/A |
| AAV5-EF1a-DIO-EYFP | UNC Vector Core | N/A |
| Experimental models: Organisms/strains | | |
| TH-Cre Long-Evans rats (LE-Tg[TH-Cre] 3.1Deis) | Rat Resource and Research Center | RRRC#: 00659; RRID: RGC_104012201 |
| Software and algorithms | | |
| MATLAB 2020b | Mathworks | RRID:SCR_001622 |
| RStudio | RStudio PBC | RRID:SCR_000432 |

### RESOURCE AVAILABILITY

#### Lead contact

Further information and requests for resources and reagents should be directed to and will be fulfilled by the lead contact, Daniel Leventhal (dleventh@med.umich.edu).

#### Materials availability

This study did not generate new unique reagents or standardized datatypes.

#### Data and code availability

Data

All data reported in this paper will be shared by the lead contact upon request.

Code

All original code is available in this paper's supplemental information.

All other items

Any additional information required to reanalyze the data reported in this paper is available from the lead contact upon request.

### EXPERIMENTAL MODEL AND SUBJECT DETAILS

The University of Michigan Institutional Animal Care and Use Committee approved all animal procedures. 15 tyrosine hydroxylase (TH)-Cre$^{+}$ Long-Evans adult rats (9 male, 6 female, obtained RRID: RGC_104012201, aged 70–155 days at the time of virus infusion), a subset of rats analyzed in a published study (Bova et al., 2020), were analyzed in this report. Rats were randomly allocated to active channelrhodopsin (ChR2) or EYFP control groups. The ChR2 group was further divided into 'primary during-reach stimulation' and 'inter-reach stimulation' groups depending on the timing of stimulation with respect to reaching (Figure 1). The 'inter-reach' group later transitioned to 'during-reach' timing ('secondary during'). Prior to optical fiber implantation, rats were housed in groups of 2-3 on a reverse light-dark cycle. Following implantation, rats were individually housed to avoid injury to the implant. Training and testing were conducted during the dark cycle. Rats were food restricted during training and testing periods except

for one day each week. Their weights were monitored to ensure that they remained within 85–90% of free-feeding weight.

## METHOD DETAILS

### Virus injections and surgeries

Surgeries were conducted under isoflurane anesthesia (5% induction, 2–3% maintenance). Prior to skilled reaching pre-training, TH-Cre + rats were bilaterally injected in the SNc (M-L ±1.8 mm; A-P −5.2 mm, −6.2 mm; D-V −7.0 mm, −8.0 mm) with AAV-EF1α-DIO-hChR2(H134R)-EFYP or AAV-EF1α-DIO-EYFP (Cre-dependent DIO AAV vectors). Each site was injected with 1 μL of virus (titer: 3.4–4.2 × $10^{12}$ vg/mL) at a rate of 0.1 μL/min, resulting in 4 μL total per hemisphere. Once rats had achieved stable skilled reaching performance, we implanted optical fibers (multimode 200 μm core, 0.39 NA, Thor Labs FT200EMT) embedded in stainless steel ferrules (2.5 mm outer diameter, 230 μm bore size, Thor Labs #SF230-10) above SNc contralateral to the rat's preferred reaching paw (M-L ±2.4 mm, A-P −5.3 mm, D-V −7.0 mm). Prior to implantation, optical fibers were calibrated to determine fiber tip optical power as a function of laser output power. After optical fiber implantation, rats recovered for at least 7 days before re-training on the skilled reaching task.

### Skilled reaching

Rats were trained and tested in a single pellet skilled reaching chamber with high-speed video capture (Bova et al., 2019, 2020; Ellens et al., 2016). A trial is initiated when rats break an IR beam in the back of the chamber, triggering an actuator to raise a sugar pellet in front of a slot at the front of the box (Figure 1D). Once this pellet is raised, the rat can reach through and attempt to grasp the sugar pellet. Two types of video recordings were made (Figure 1B). The first were 4.3 s, 300 fps videos triggered by each reach that allowed detailed analysis of individual reaches. The second was a full-session recording made with a commercial camcorder at 60 fps (HC-V110, Panasonic) from the top of the chamber. This allowed us to analyze behavior when the rat was not actively reaching.

During pre-training, rats were familiarized with the reaching chamber, evaluated for paw preference, trained to reach, and trained to request a pellet by moving to the back of the chamber (Bova et al., 2020). After pre-training, rats performed 30-min training sessions 6 days per week with the full automated system. Once rats performed at least 35 reaches per session at a success rate above 40% for three sessions, they were implanted with optical fibers.

### Optogenetics

After implantation, rats were re-trained for 10 days with the patch cable attached but stimulation off to acclimate to the tether (Figure 1A – "retraining"). ChR2 rats were divided into two groups based on timing of optogenetic stimulation: 'primary during' and 'between'. In the 'primary during' group, the laser turned on when the rat broke the IR beam and off 3 s after the video trigger (Figure 1D). In the 'between' group, the laser turned on 4 s after the video trigger and off 5 s later. The duration of 'between' and 'during' stimulation was comparable, with a median duration of 5.37 s for 'during' compared to 5 s for 'between' (Bova et al., 2020). 473 nm laser light (Opto Engine DPSS laser) was delivered to all rats at an estimated 20 mW at the fiber tip and 20 Hz using an optical chopper (Thorlabs MC1F10HP). Power was estimated at the fiber tip using measurements of transmission power with a calibrated photodiode prior to surgical implantation (Thorlabs S121C connected to Thorlabs PM100D Power Meter).

### Dopamine neuron stimulation in the cylinder context

Stimulation was delivered to rats in a clear plexiglass cylinder (diameter = 21 cm) with mirrors on two sides allowing visibility from multiple angles (Figures 4A and 4B). Testing occurred one day before the first day of retraining (Figure 1A, 'pre-reaching') and one day after the last day of occlusion sessions ('post-reaching'). Comparisons between pre-reaching and post-reaching cylinder tests are published and not repeated here (Bova et al., 2020). Here, the key comparisons are between the 'post-reaching' cylinder data and AIMs in the skilled reaching chamber. Rats were attached to the patch cable and stimulated with the laser for a series of 30 s on/30 s off periods. Sessions began with a rest period, and then laser power was varied in a pseudo-random order (5, 10, 15, 20, or 25 mW estimated at the fiber tip). Stimulation was applied at 20 Hz. Only the 20 mW laser power was included in this analysis to compare with 20 mW, 20 Hz stimulation during reaching sessions. Cylinder sessions were recorded at 60 frames per second (HC-V110, Panasonic).

### AIMs scoring

AIMs were scored for severity utilizing an established scale. Amplitude scores range from 0 (normal) to 4 (severe), indicating the "degree of deviation of dyskinetic body parts from their resting position" (Sebastianutto et al., 2016). Each trial was assigned an axial (A0-A4) and limb score (L0-L4). Global AIMs scores were calculated by summing the axial and limb amplitude scores. Typically, levodopa-induced AIMs are also scored for their duration. However, we did not give duration scores because that was determined by the length of optogenetic stimulation.

### Behavioral conditions

Three conditions were scored: 'non-reaching', 'reaching', and 'cylinder' (Figures 1C and 1D).

'Non-reaching' occurred during 30-min sessions in the skilled reaching chamber for all groups ('primary/secondary during', 'between', and 'control'). Each stimulation period received an axial and limb score, but only when the rat was not actively reaching. For 'during' and 'control' rats, which received stimulation from beam break to 3 s after video trigger, AIMs were scored during the entire stimulation epoch except during active reaching as judged by the scorer. That is, AIMs were evaluated both before and after each reach. 'Between' rats were scored for their entire stimulation periods. The reviewer was blinded to the rat's virus (ChR2 or EYFP-only) and day of testing. Global AIMs scores were calculated for each stimulation epoch and averaged across each 30-min session.

'Reaching' was when rats were actively reaching. This was analyzed exclusively for 'primary during' and 'control' rats to determine if AIMs were present during reaches. We randomly selected ten unsuccessful (did not obtain pellet) day 10 reach trials for each rat (Bova et al., 2020). Reviewers were blinded to virus and session number. Limb and axial AIMs scores were assigned based on observation of reach disruptions from the front of the chamber (Figure 1B). Global AIMs scores were calculated for each session and averaged across rats. These data have been reported (Bova et al., 2020), but here are compared to 'non-reaching' day 10 scores, which are new. 'Between' rats did not receive stimulation during the reach, so AIMs were not evaluated during their reaches.

The 'cylinder' condition describes behavior during the 'post-reaching' cylinder session. This evaluated effects of dopamine neuron stimulation in a novel context. All cylinder sessions were segmented into individual videos for each 30 s period and blinded for virus and laser power. Axial and limb AIMs were scored for amplitude, and the global AIMs score was calculated. After scoring, sessions at a power of 20 mW were selected. One 'control' rat was not tested in the cylinder context. These data have been reported (Bova et al., 2020). Here they are compared to "non-reaching" AIMs scores, which are new (but scored by the same reviewer).

### Immunohistochemistry

Immunohistochemistry was performed to verify viral expression in dopamine neurons and optical fiber placement above SNc, as documented previously (Bova et al., 2020). Rats were anesthetized and perfused with paraformaldehyde. Their brains were removed, fixed, and rinsed with saline. 30 μm sagittal sections were taken around SNc where the optical fiber was visible on a cryostat (Leica Microsystems). Immunohistochemistry was performed for TH and EYFP (Bova et al., 2020). Slices were imaged with an Axioskops 2 Plus microscope fitted with an Olympus DP72 camera. Slides were re-imaged using a Leica Stellaris confocal microscope for publication.

Images were evaluated by two individuals blinded to behavioral outcomes. Sections were evaluated for virus expression in SNc and striatal dopamine fibers, and location of the fiber tip over SNc. Rats with inadequate expression or misplaced fibers were excluded from analysis (number of rats excluded - during: n = 1; between: n = 3; control: n = 0. This left the 15 rats described above).

## QUANTIFICATION AND STATISTICAL ANALYSIS

Linear mixed-effects models evaluated AIMs amplitude across sessions. We implemented linear mixed-effects models (R *lmer*) with random intercepts/effects for each rat and a main effect of session number. This analysis was done for each group: 'during-reach,' 'inter-reach,' and 'control,' as well as a combination of 'inter-reach and 'during-reach' (all ChR2). Furthermore, to determine if AIMs were significantly different

between 'during-reach' and 'inter-reach' groups, a linear mixed model was implemented (R *lmer*) with random intercepts/effects for each rat and main interaction effects of session number and group ('during-reach' or 'inter-reach').

Differences in AIMs scores between behavioral contexts (i.e., reaching vs non-reaching) were tested with the Wilcoxon Signed-Rank test (MATLAB *signrank*).

To determine if AIMs scores varied between physical contexts (reaching chamber vs cylinder), we compared day 10 'non-reaching' AIMs scores to the 'cylinder' with Wilcoxon Signed-Rank tests (MATLAB *signrank*).